



Analysis

<https://doi.org/10.1038/s44220-025-00503-6>

The network-based underpinnings of persisting symptoms after concussion: a multimodal neuroimaging meta-analysis

Received: 27 August 2024

Accepted: 19 August 2025

Published online: 23 September 2025

Check for updates

Adriano Mollica 1,2,12, Robin F. H. Cash 3,4,12, Carl Froilan D. Leochico^{5,6}, Peter Giacobbe^{1,2}, Isabella J. Sewell¹, Andrew Zalesky 3,4, Jennifer S. Rabin 1,7, Maged Goubran 1,8,9, Simon J. Graham^{8,9}, Benjamin Davidson^{1,10}, Fa-Hsuan Lin^{8,9}, Nir Lipsman^{1,10}, Clement Hamani 1,10, Matthew J. Burke^{1,2,11,13} & Sean M. Nestor 1,2,13

Persisting symptoms after concussion (PSaC) represent a complex and poorly understood neuropsychiatric phenomenon with limited treatment options. Neural network dysfunction has been associated with PSaC, and neuromodulation, particularly repetitive transcranial magnetic stimulation, may be a promising intervention. However, neuroimaging findings have been inconsistent, limiting understanding of underlying network dysfunction. We aimed to identify a core neural network associated with PSaC and explore whether this network could yield candidate cortical targets for neuromodulation at the individual level. We hypothesized that differences in network disruption would be evident between individuals with high versus low symptom burden in PSaC. Here we show that a convergent multi-analytic approach combining symptom–activation maps generated from existing fMRI datasets, systematic review of resting-state fMRI studies of PSaC, and network-based meta-analysis of coordinates derived from these studies co-localize to the salience network in high symptom burden PSaC. Using Human Connectome Project data, we mapped this network to cortical regions that could serve as individualized targets for neuromodulation. This aligns with current clinical models of PSaC and may present a new direction for network-based therapy.

Persisting symptoms after concussion (PSaC) (formerly referred to as post-concussive syndrome) represents a complex neuropsychiatric phenomenon that occurs in 10–30% of patients¹. It is characterized by a disparate range of physical, cognitive and emotional symptoms, persisting for at least 4 weeks beyond the acute phase of injury^{2,3}. The polysymptomatic nature of PSaC and lack of objective biomarkers necessitate a multipronged, symptom-targeted treatment approach⁴. Current clinical guidelines emphasize a multidisciplinary framework that includes individualized management of symptoms such as

headache, depression, vestibular dysfunction, cognitive impairment and fatigue, often involving a combination of physical therapy, cognitive rehabilitation, pharmacological treatments and psychological interventions^{5,6}. Within PSaC, there is substantial heterogeneity regarding the degree of neurological insult, mechanism of injury, symptom presentation, duration and perceived severity, as well as predisposing and perpetuating biopsychosocial factors^{5,7,8}. Key risk factors for a high burden of persisting symptoms include female sex, non-white ethnic groups, substance use, pre-existing psychiatric conditions, history of

A full list of affiliations appears at the end of the paper. e-mail: sean.nestor@utoronto.ca

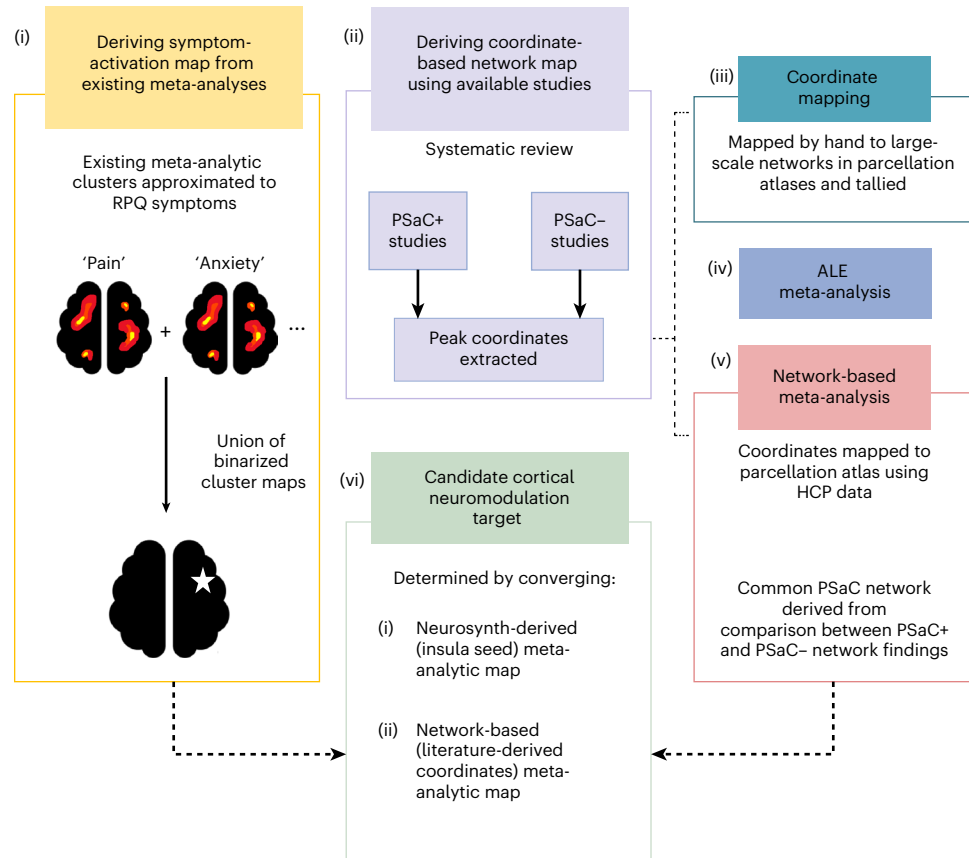


Fig. 1 | Flow diagram of neuroimaging analyses. A converging multi-analytical approach was used to explore network dysfunction in PSaC that included (i) generation of symptom-activation maps from existing fMRI datasets available on Neurosynth to identify common areas of activation across PSaC symptoms; (ii) systematic review of PSaC neuroimaging studies to contrast network alterations in those with high versus low symptom burden after concussion; (iii) mapping and tallying extracted coordinates individually to large-scale

networks in parcellation atlases; (iv) Activation Likelihood Estimation (ALE) meta-analysis of included studies using a seed-based connectivity approach; (v) network-based meta-analysis of coordinates derived from whole-brain connectivity to contrast high versus low symptom burden patterns of altered connectivity; and (vi) determination of a functional cortical signature for neuromodulation targeting with Human Connectome Project (HCP) data.

chronic pain and history of somatization. These sources of variability challenge the notion of a uniform pathophysiological mechanism to explain PSaC^{4,9–11}. However, the answer to why some individuals develop persisting symptoms while others recover may be rooted in large-scale neural network dysfunction^{12–14}. Advances in neuroimaging and image-guided neuromodulation offer new avenues for measuring and targeting these network dysfunctions, which could be a meaningful addition to the toolbox of management strategies for PSaC^{15,16}.

Symptom perpetuation in PSaC has been linked to heightened vigilance and attentional bias toward bodily sensations, negative attributions and fear-driven avoidance^{17–19}. At a neural level, these processes are probably mediated by dysfunction in large-scale networks involved in sensory processing, attentional control and cognitive-emotional integration, particularly the salience network, executive-control network, default-mode network and somatomotor network^{20–24}. Disruptions across these networks have been associated with PSaC, with altered connectivity patterns linked to symptom severity, impaired cognitive control and emotional dysregulation^{23,25,26}. Heightened interactions between sensory processing regions and attentional networks suggest a maladaptive reinforcement of symptom perception^{14,27}, while increased connectivity within cognitive control networks may represent compensatory mechanisms that ultimately contribute to inefficiencies and cognitive symptoms^{22,25}. Despite these insights, it remains unclear whether dysfunction in a specific network plays a dominant role in driving the polysymptomatic presentations associated with PSaC^{12,20}. Given the potential for network-based interventions, such

as neuromodulation, a clearer understanding of the neural correlates underlying PSaC could provide critical insights for targeted treatment strategies¹⁵.

Neuromodulation approaches that directly target functional brain networks, such as repetitive transcranial magnetic stimulation (rTMS), have demonstrated mixed results for treating PSaC^{28,29}. Two studies have evaluated the effects of left dorsolateral prefrontal cortex (DLPFC) rTMS on global symptoms of PSaC^{30,31}. While one open-label pilot study reported a large effect size (Cohen's $d = 0.91$)³⁰, a double-blind sham-controlled trial found no therapeutic benefit compared with sham stimulation³¹. These previous rTMS studies targeted the DLPFC due to its central role in cognitive control networks and its established use in depression treatment^{28,32}. However, depression accounts for a substantial portion of the experience of PSaC and shares overlapping neural mechanisms, making it difficult to disentangle the effects of DLPFC rTMS on mood from its potential impact on other PSaC-related symptoms^{33–36}. This challenge underscores the need for a more mechanistically driven approach that accounts for individual network dysfunction rather than relying on anatomical targets derived from other conditions^{16,28}. Establishing a clearer understanding of the neural mechanisms underlying PSaC may help optimize network-based neuromodulation strategies and expand treatment options.

In this study, we aimed to (1) identify a core neural network from functional magnetic resonance imaging (fMRI) associated with PSaC and (2) explore whether this network could yield candidate cortical

targets for neuromodulation at the individual level. We hypothesized that differences in network disruption would be evident between individuals with high versus low symptom burden in PSaC. High versus low symptom burden was determined on the basis of the primary clinical outcome measures used in each study, including predefined cut-off scores, categorical distinctions (for example, severity ratings of specific symptoms) or, when a clear cut-off score was not defined, classification was based on whether the total score at the time of neuroimaging assessment was above or below recognized thresholds for the measure being used. Leveraging a multi-faceted set of neuroimaging analyses across different data sources (Fig. 1), we identified the network-based underpinnings of PSaC and localized an optimal candidate target for neuromodulation therapies.

Results

PSaC symptom-based network mapping

To identify a functional network clinically relevant to PSaC, we approximated 11 symptoms from the Rivermead Post-Concussion Questionnaire (RPQ) to available homologous terms in the Neurosynth database and extracted their corresponding meta-analytic activation maps (Fig. 2a). The union of 11 RPQ symptom–activation maps revealed an overlapping activation pattern that co-localized specifically to salience network topology, which was anchored by the right insula (Montreal Neurological Institute (MNI) coordinates 34, 21, 0) and left insula (MNI coordinates -35, 20, 0; Fig. 2b). As the Neurosynth-derived symptom maps did not primarily include studies of traumatic brain injury (TBI) or concussion patients, we conducted a separate coordinate-based meta-analysis using Neurosynth Compose, filtering for studies specifically involving participants with concussion ($n = 37$). The resulting activation map was binarized and multiplied with the RPQ symptom–activation map, which revealed consistent localization to the bilateral anterior insula (Supplementary Fig. 1).

Systematic review of PSaC resting-state-based network mapping

To further investigate the neural networks implicated in PSaC, we conducted a systematic review of neuroimaging studies using resting-state fMRI that provided MNI coordinates for analysis. In addition to identifying common network alterations associated with PSaC, we sought to determine whether these patterns differed between individuals with high symptom burden (PSaC+) and those with low symptom burden or who had recovered (PSaC-).

A Preferred Reporting Items for Systematic Reviews and Meta-Analyses (PRISMA) flow diagram is presented in Supplementary Fig. 2. In total, 19 studies consisting of 1,300 unique participants met eligibility criteria. Group-wise demographic details, pertinent results and neuroimaging details are reported in Table 1 and Supplementary Tables 1 and 2, respectively. The proportion of female participants was 46.5% in PSaC+ studies, 45.4% in PSaC- studies and 26% in the two studies that included both groups. The mean and median time between injury and neuroimaging assessment was 28.3 and 10.2 months for PSaC+ studies and 6.6 and 5.0 months for PSaC- studies. Six out of 12 PSaC+ studies and 2 out of 5 PSaC- studies (as well as both studies comparing high and low symptom burden) excluded psychiatric conditions. Only 3 out of 12 PSaC+ studies and 1 out of 5 PSaC- studies (along with both high versus low symptom burden studies) excluded participants with a previous history of concussion (Supplementary Table 3).

Across studies, there was variability in the use of clinician-rated versus self-reported measures to assess symptom burden. In the PSaC+ group, 6 out of 12 studies used clinician-rated measures, with an additional two studies incorporating both clinician- and self-rated measures, whereas 2 out of 5 PSaC- studies used clinician-rated measures (Table 1).

Several PSaC+ studies explicitly diagnosed post-concussive syndrome (PCS) (that is, the former term for PSaC) using criteria such as the tenth revision of the International Statistical Classification of

Diseases and Related Health Problems (ICD-10)^{15,37–39} or *Diagnostic and Statistical Manual of Mental Disorders* fourth edition (DSM-IV)²⁷, while others relied on predefined cut-off scores from their clinical outcome measures^{40–45}. Three PSaC+ studies did not specify a cut-off score for symptom burden, but the scores in these studies for the PSaC patients were above suggested symptom severity thresholds in the literature (Supplementary Table 4)^{26,46,47}.

PSaC- studies were primarily recovery-focused, tracking considerable improvements in primary clinical outcomes over time. At the time of neuroimaging assessment, their reported clinical outcome scores were below established cut-off thresholds for high symptom burden, including the RPQ^{48–54}, Sport Concussion Assessment Tool – 3rd Edition^{51,52,55,56}, Glasgow Outcome Scale–Extended^{53,57}, and Hamilton Depression Rating Scale (HAM-D)^{54,58}. Two studies explicitly compared high versus low symptom burden within PSaC+ groups using categorical criteria: one study categorized participants on the basis of self-reported mild versus severe headache⁵⁹, while another distinguished between those with and without cognitive symptoms on the RPQ³⁹.

In the quality assessment of the included studies, 15 of 19 were considered good quality, while 2 of 19 were deemed fair quality (1 PSaC+ and 1 PSaC- study), and 2 of 19 were rated as poor quality (both PSaC+ studies; Supplementary Tables 5 and 6). Notably, none of the included studies provided commentary on sample size justification or power description.

Statistical analysis of coordinates derived from systematic review

A total of 177 coordinates were extracted from PSaC+ studies, compared with 67 coordinates from PSaC- studies. This difference reflects both the relatively higher number of PSaC+ studies included in the analysis and variability in the number of reported MNI coordinates across individual studies. All coordinates represented altered functional connectivity changes compared with a control group, and coordinates were pooled regardless of the resting-state fMRI methods used. In PSaC+ studies, most extracted coordinates aligned with the salience network (46, 26%), followed by default-mode network (30, 17%), visual network (28, 16%), dorsal attention network (19.5, 11%), executive-control network (17, 10%), somatomotor network (14, 8%) and limbic network (6.5, 4%). For the PSaC- studies, most extracted coordinates aligned with the default-mode network (19, 28%), followed by executive-control network (14, 21%), salience network (14, 21%), dorsal attention network (4, 6%), somatomotor network (5.5, 8%), visual network (3.5, 5%) and limbic network (4, 6%). Coordinates in the thalamus, cerebellum and midbrain could not be reliably assigned to a network for PSaC+ and PSaC- groups. We found a similar pattern of results when examining the Yeo and Schaefer atlases (80% and 83% concordance between atlases for PSaC+ and PSaC-, respectively).

Across groups, widespread multi-network changes were observed following concussion/mild TBI (mTBI; Fig. 2c). The largest difference between PSaC+ and PSaC- studies was in the salience network, with 14 of 14 (100%) of PSaC+ studies showing functional network changes compared with 4 of 7 (57%) of PSaC- studies ($P = 0.026$). Non-significant differences were also observed in the dorsal attention network (79% versus 57%, $P = 0.24$) and visual network (50% versus 29%, $P = 0.25$). The default-mode network (12 of 14, 86% versus 6 of 7, 86%, $P = 0.48$), executive-control network (12 of 14, 86% versus 6 of 7, 86%, $P = 0.48$), somatomotor network (6 of 14, 43% versus 3 of 7, 43%, $P = 0.36$) and limbic network (4 of 14, 29% versus 3 of 7, 43%, $P = 0.30$) demonstrated similar patterns of network alteration between PSaC+ and PSaC- studies.

We next explored patterns of reported functional connectivity between the salience network and other large-scale networks in PSaC+ versus PSaC- studies. Within PSaC+ studies, 17% of salience network coordinates reported connectivity with the executive-control network, 5% with the dorsal attention network and 8% with the sensorimotor

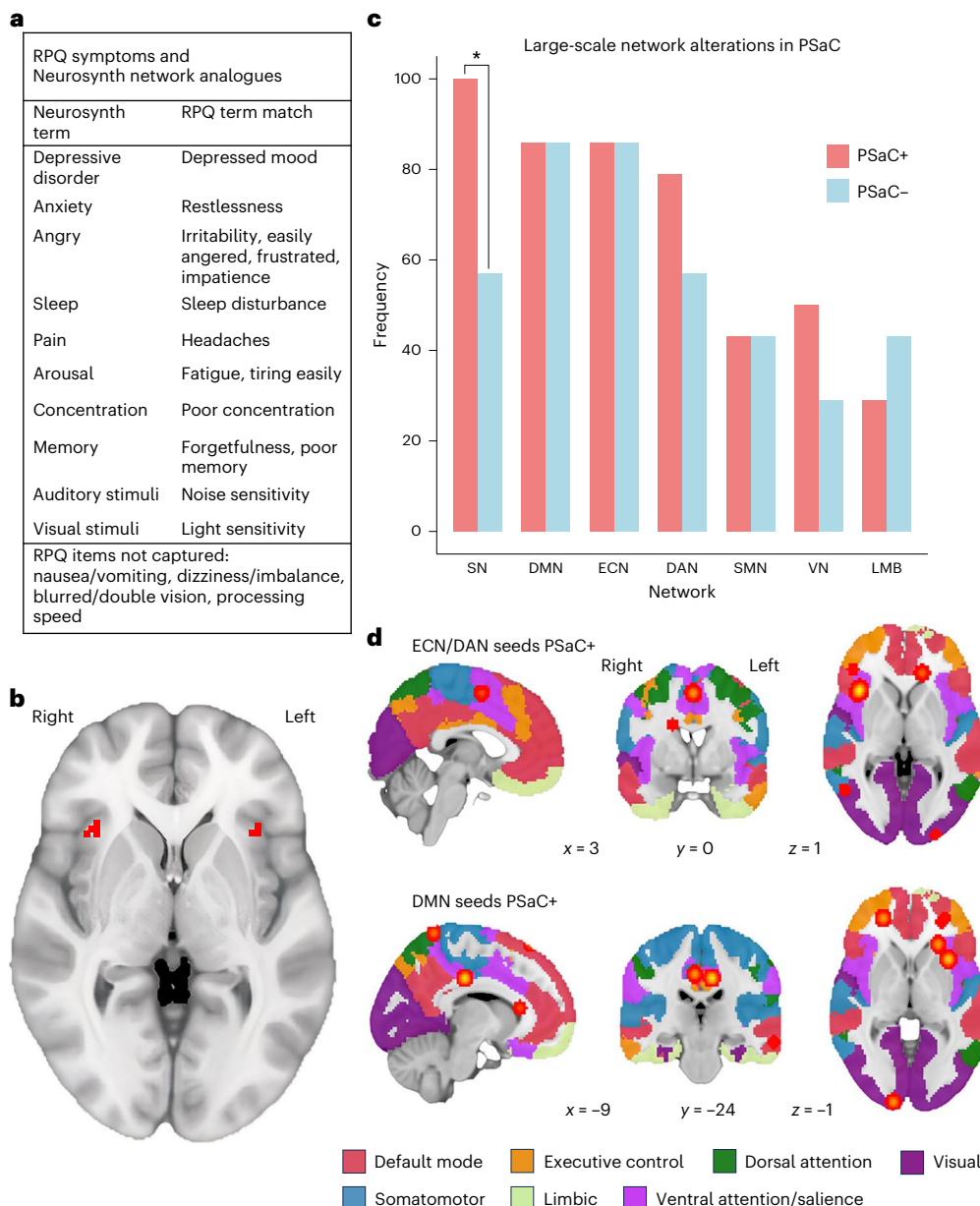


Fig. 2 | PSaC symptom-based map and coordinate-based analyses. **a**, RPQ symptoms and Neurosynth functional network analogs. **b**, Symptom–activation map derived from Neurosynth data, showing the union of 11 RPQ-derived terms with bilateral insula activation. **c**, Alterations across large-scale networks in PSaC+ versus PSaC– studies determined by network mapping on parcellation atlases. The only significant difference found between groups was in the salience network (* $P=0.026$, Fisher's exact test). **d**, Unthresholded and non-significant

ALE image results of activations/increased connectivity between seeds in the executive-control network (ECN)/dorsal attention network (DAN) (top panel), default-mode network (DMN) (bottom panel), and peak regions in PSaC+ studies. Cross sections provided are core regions of the salience network (bilateral insula and dorsal anterior cingulate cortex). Each image is overlaid on the MNI 152 brain with Yeo 2011 7-network parcellation atlas. LMB, limbic network; SMN, somatomotor network; SN, salience network; VN, visual network.

network. By contrast, 12% of salience network coordinates in PSaC– studies reported connectivity with the limbic network, compared with 4% in PSaC+ studies. The proportion of salience network coordinates linked to the default-mode network (33% versus 35%) and the visual network (10% versus 12%) was similar across both groups. These values reflect descriptive trends only, as no statistical comparisons were performed (Supplementary Table 7).

In summary, PSaC+ studies demonstrated widespread multi-network changes, with the most consistent alterations observed in the salience network, which was significantly more affected than in PSaC– studies ($P=0.026$). While non-significant differences were noted in other networks, connectivity analyses further revealed that PSaC+ studies more frequently reported increased functional connectivity

between the salience network and executive-control, dorsal attention and somatomotor networks.

Coordinate-based meta-analysis of seed-based connectivity studies

Given the limited number of studies suitable for activation-likelihood estimation (ALE) analysis in PSaC– studies, we examined peak coordinates from PSaC+ studies using the executive-control network/dorsal attention network or default-mode network network as seed locations, as these were most represented across studies (6 studies with 32 coordinates using executive-control network/dorsal attention network seeds, and 5 studies with 23 coordinates using default-mode network seeds). ALE meta-analysis of studies using whole-brain fMRI analyses in

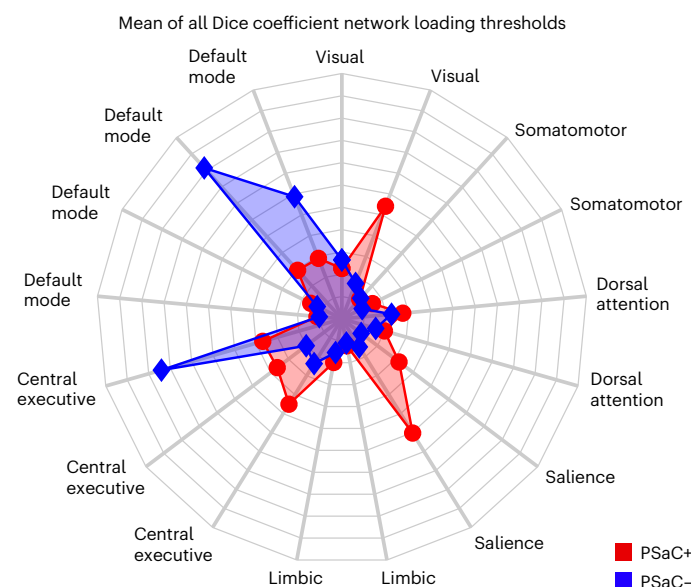
Table 1 | Characteristics of included studies

Study	Design	Sample size (mTBI, healthy controls)	Percentage female	Nature of mTBI	Mean symptom duration (months)	Primary symptom domain	Diagnostic approach to PSaC	Primary clinical outcome measure	Cut-off score	Clinician rated or self-rated
PCS+ studies										
Amir 2021 (ref. 40)	Cross-sectional	53 (27, 26)	70	Civilian	8.8	Global	Cut-off score	RPQ	RPQ \geq 30	Self-rated
Dumkrieger 2019 (ref. 37)	Case-control	80 (44, 36)	36	Mixed	108	Headache	Headache specialist assessment	Numeric rating scale	ICDH-3 diagnostic criteria	Clinician rated
Leung 2016 (ref. 41)	Cross-sectional	30 (15, 15)	26	Veteran	70	Headache	Headache specialist assessment	Numeric rating scale, visual analog scale	ICDH-2 diagnostic criteria+visual analog scale score \geq 3 out of 10	Clinician+ self-rated
Rockswold 2019 (ref. 42)	Longitudinal	19 (10 PCS+ and 9 PCS-)	53	Civilian	3	Vision	Vision testing by optometrist	Optometric testing	Determined to have substantial oculomotor dysfunction	Clinician rated
Runyan 2022 (ref. 44)	Cross-sectional	127 (46, 81)	7	Veteran	11.6	Cognition	Cut-off score	NSI	Score of \geq 3 on any NSI cognitive symptoms	Clinician rated
Shafi 2020 (ref. 27)	Cross-sectional	111 (80, 31)	33	Civilian	19	Global	Diagnostic assessment	DSM-IV PCS diagnostic criteria	DSM-IV PCS diagnostic criteria	Clinician rated
Sheth 2021 (ref. 43)	Cross-sectional	74 (49, 25)	10	Veteran	144	Post-traumatic stress disorder	Cut-off score	Clinician-Administered Post-traumatic Stress Disorder Scale	CAPS cut-off (score of \geq 2)	Self-rated
Sours 2015 (ref. 45)	Longitudinal	56 (28, 28)	33	Civilian	6	Global	Cut-off score	RPQ	\geq 3 RPQ symptoms present at 3months	Self-rated
Stevens 2012 (ref. 46)	Cross-sectional	60 (30, 30)	33	Civilian	2	Global	Total score, no cut-off ^a	Post-concussion symptoms checklist	No cut-off used; scores well above recognized threshold	Self-rated
Trofimova 2021 (ref. 47)	Longitudinal	22 (12, 10)	92	Mixed (civilian + sports)	2	Vestibular	Total score, no cut-off ^a	Post-Concussion Symptom Scale+Vestibular/Ocular Motor Screen	No cut-off used; scores well above recognized threshold	Clinician+ self-rated
Vedaei 2023 (ref. 38)	Cross-sectional	100 (60, 40)	62	Civilian	24	Global	Diagnostic assessment	ICD-10 PCS diagnostic criteria	ICD-10 PCS diagnostic criteria	Clinician rated
Wong 2023 (ref. 26)	Cross-sectional	38 (17, 21)	100	Civilian	21.5	Global	Total score, no cut-off ^a	Composite score of Graded Symptom Scale Checklist severity and cognitive testing	No cut-off used	Clinician rated
PCS- studies										
Chong 2019 (ref. 51)	Longitudinal	30 (15, 15)	87	Civilian	5	Global	Total score, no cut-off ^a	Sport Concussion Assessment Tool 3	No cut-off used	Self-rated
Churchill 2019 (ref. 52)	Longitudinal	146 (24, 122)	50	Sports	12	Global	Total score, no cut-off ^a	Sport Concussion Assessment Tool 3	No cut-off used	Self-rated
De Souza 2020 (ref. 53)	Longitudinal	39 (39, 0)	26	Civilian	18	Global	Total score, no cut-off	Glasgow Outcome Scale-Extended	No cut-off used	Clinician rated
D'Souza 2020 (ref. 48)	Longitudinal	120 (60, 60)	43	Civilian	6	Global	Total score, no cut-off	RPQ	No cut-off used	Self-rated
McCuddy 2018 (ref. 54)	Longitudinal	94 (43, 51)	21	Sports	1	Mood	Total score	HAM-D	HAM-D cut-off scores	Clinician rated

Table 1 (continued) | Characteristics of included studies

Study	Design	Sample size (mTBI, healthy controls)	Percentage female	Nature of mTBI	Mean symptom duration (months)	Primary symptom domain	Diagnostic approach to PSaC	Primary clinical outcome measure	Cut-off score	Clinician rated or self-rated
Studies that distinguished between high-symptom and low-symptom groups										
Flowers 2021 (ref. 59)	Cross-sectional	64 (16 PCS+ and 16 PCS-, 32)	0	Veteran	3	Headache	Categorical cut-off score	NSI	Headache severity rating (mild (1), moderate (2), severe (3 or 4))	Self-rated
Sours 2013 (ref. 39)	Cross-sectional	37 (13 PCS+ and 10 PCS-, 14)	52	Civilian	1	Cognition	Diagnostic assessment + categorical cut-off score	RPQ	ICD-10 PCS diagnostic criteria + presence of cognitive symptoms on RPQ (that is, yes/no)	Clinician + self-rated

NSI, Neurobehavioral Symptom Inventory. ^aTotal score was used in neuroimaging analysis.

**Fig. 3 | Relation between coordinates and large-scale networks in PSaC.**

By calculating the mean of absolute z scores for each Yeo network and applying Dice coefficients to the Z maps generated from whole-brain analyses of PSaC+ and PSaC- studies, a predominant overlap of coordinates is observed in PSaC+ studies with the salience network, in contrast to coordinates from PSaC- studies.

PSaC+ with a control group (nine studies) did not reveal a statistically significant cluster of activation or deactivation when examining peak coordinates from executive-control network/dorsal attention network or default-mode network seeds. However, unthresholded ALE maps of peak coordinates from these network seeds demonstrated selective overlap with the salience network, including the bilateral insula and dorsal anterior cingulate cortex, when overlaid on the Yeo 7-network parcellation atlas (Fig. 2d).

Computation of connectivity and brain networks

A network-based meta-analytic approach resulted in a robustly distributed brain network in PSaC+ that mapped primarily onto the salience network, executive-control network and visual network (Fig. 3 and Supplementary Fig. 3). By contrast, the network derived from PSaC- mapped predominantly onto the default-mode network and executive-control network.

Deriving a network candidate for neuromodulation

Whereas the connectivity map derived from bilateral insula seeds using Neurosynth data (that is, the symptom–activation map) revealed sites of maximal correlation in the DLPFC, these locations were notably different in location from areas of maximum activation in the DLPFC generated by the network meta-analytic approach from PSaC+ studies (Fig. 4 and Supplementary Fig. 4). While the convergence map highlights potential regions of interest for neuromodulation (Fig. 4), these findings should be interpreted with caution given the broad functional role of the DLPFC and its involvement in both cognitive and affective processes. Further investigation is necessary to refine candidate targets.

Discussion

Given the lack of convergent findings across neuroimaging literature for individuals experiencing persistent symptoms after concussion/mTBI, we aimed to (1) identify a core neural network associated with PSaC and (2) consider whether this network could be targeted at the individual level with neuromodulation. Previous work has shown that multiple systems are altered in both PSaC- and PSaC+ following concussion/mTBI. Using a converging multi-analytic approach, we identified the salience network as a core network that appears to be disproportionately altered in PSaC+. Systematic review of seed-based and region-of-interest (ROI) studies also revealed increased functional connectivity between the salience network and other large-scale systems, including the executive-control network, dorsal attention network and somatomotor network, that was not observed in PSaC-. This was further corroborated by network-based meta-analysis of peak coordinates that strongly implicate salience network dysconnectivity in PSaC+, as opposed to more prominent executive-control network and default-mode network changes seen in PSaC- studies (Fig. 3 and Supplementary Fig. 3). This underscores the importance of the salience network and network-level considerations in understanding the pathophysiology of PSaC. To investigate personalized treatment approaches for PSaC, we used the salience network regions derived from the PSaC symptom–activation analysis to locate connected cortical regions amenable to non-invasive brain stimulation (Fig. 4). A DLPFC region displaying maximal connectivity to these ROIs was robustly identified, aiding in the determination of an optimal candidate target for delivering personalized brain stimulation treatment in PSaC trials.

The salience network^{60,61}, also known as the cingulo-opercular network⁶², ventral attention network⁶³ or midcingulo-insular network⁶⁴, has been described as a ‘neural crossroads’ due to its extensive connectivity and influence on other networks⁶⁵. Functionally, it plays a central role in perceiving and responding to internal signals and

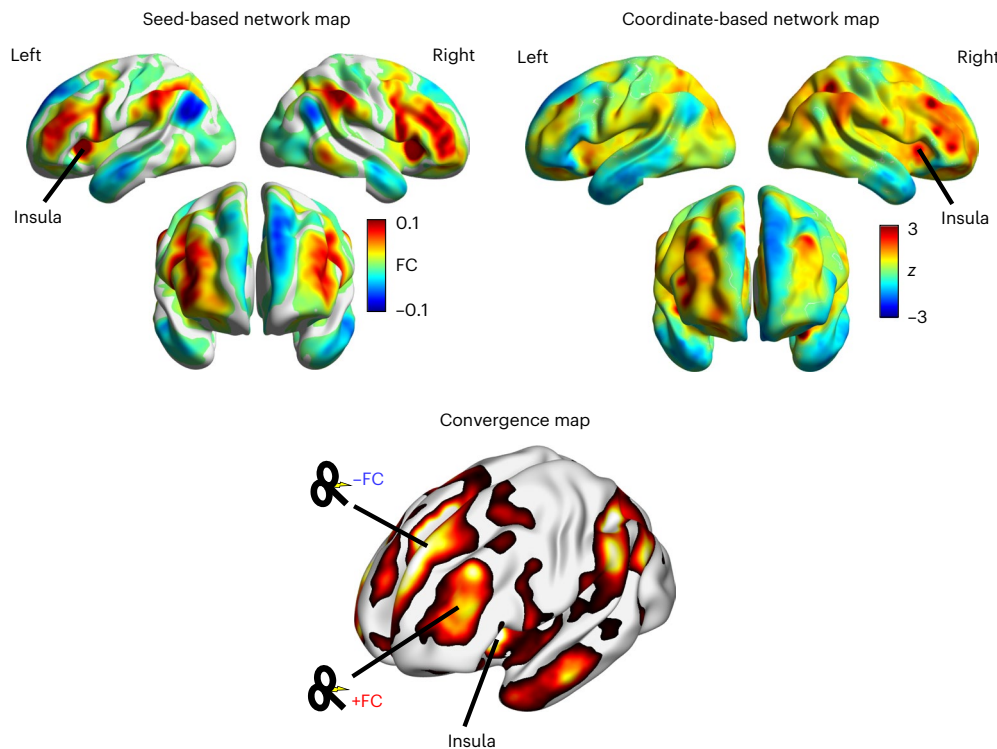


Fig. 4 | Determining candidate cortical target locations for neuromodulation.

The seed-based/symptom–activation network map depicts a network map derived from existing fMRI datasets using Neurosynth. It highlights cortical areas with maximal correlation (warm colors) and anticorrelation (cool colors) with bilateral anterior insula seeds (coordinates: 34, 21, 0 for the right and −35, 20, 0 for the left). The coordinate-based network map represents a meta-analysis of coordinates derived from whole-brain connectivity PSaC+ studies. The map showcases cortical regions where network alterations are most pronounced in post-concussive syndrome (in particular, the DLPFC). The convergence map

was created by voxel-wise multiplication of Neurosynth-derived seed-based and coordinate-based network meta-analytic maps, such that when the product of multiplication is positive it demonstrates convergence. Positive regions of agreement are indicated. Note that regions where there was no convergence were typically areas of weak functional connectivity or low z scores (that is, areas that were already not strongly implicated in either map). Two broad potential prefrontal target areas for neuromodulation are depicted. These maps can be used as seed maps to derive individual stimulation targets, as per refs. 91,114. DLPFC, dorsolateral prefrontal cortex; FC, functional connectivity.

orchestrating shifts in attention when the importance of signals changes^{66,67}. Core network regions include the anterior insula and anterior midcingulate cortex, with additional cortical (for example, supramarginal gyrus, temporoparietal junction and a component of the middle frontal gyrus) and subcortical structures (for example, amygdala, hypothalamus, putamen, caudate, nucleus accumbens and periaqueductal gray) contributing to its function^{61,67}. Dysfunction of this network has emerged as a consistent transdiagnostic feature across neuropsychiatric disorders^{65,68,69}, and efficacy of non-invasive brain stimulation methods, such as rTMS in treatment-resistant depression, has recently been associated with connectivity changes in the salience network^{70,71}. Abnormalities in the salience network have been linked to transdiagnostic neuropsychological factors, such as somatosensory amplification^{72,73}, hyperarousal-associated insomnia⁷⁴, fear-avoidance behavior⁷⁵ and mismatch between self-appraisals of objective cognitive performance and symptom reporting⁷⁶, which have been identified as relevant predisposing/perpetuating factors in PSaC^{7-9,18,77}. Furthermore, it has been postulated that initial symptoms induced by concussion (for example, dizziness, headache, fatigue, mood dysregulation and cognitive difficulties), which are typically transient, may get amplified and sustained in the subset experiencing PSaC due to excess attention on physical symptoms¹⁹. The neurophysiological role of the salience network is well positioned to be a critical mediator of such a process^{66,76,78}; however, whether this may be due to pre-existing network vulnerabilities, network changes induced by the concussion or a combination of both, remains incompletely understood.

The first part of this study involved spatially combining functional PSaC symptom maps that approximated to RPQ clinical symptoms. The

union of these maps converged within the salience network (Fig. 2b). PSaC symptom maps were derived from a symptom-based approach rather than an etiological-based approach, meaning they were not based exclusively on TBI populations. However, the convergence of multiple different functions on the salience network, whether related to TBI specifically or not, implicates a multimodal sensory processing and integrative nexus that may be particularly vulnerable to post-injury remodeling⁷⁹. To improve specificity, we conducted a coordinate-based meta-analysis using Neurosynth Compose, filtering for studies that included exclusively participants with concussion. The resulting binarized activation map was intersected with the union of the 11 RPQ symptom–term activation maps, ensuring that only co-localizing regions were retained. This confirmed that the identified areas of activation remained co-localized to the bilateral insula and salience network, reinforcing the relevance of this network to PSaC.

PSaC studies from our systematic review, where salience network dysfunction was identified, involved a range of symptoms, such as pain/headache^{37,41,59}, vestibular and visual symptoms^{42,47}, cognition^{39,44} and mood symptoms⁴³, with the remainder involving global symptom burden measured by PSaC symptom questionnaires^{26,27,38,40,45,46}. Although not a focus of our study, early post-injury changes in salience network structures may potentially differentiate those who develop chronic symptoms from those who recover^{23,74,76,78,80}. Recent research by Woodrow et al.¹⁴ implicated early functional alterations in the right ventral anterior and ventrolateral dorsal thalamic nuclei as distinguishing factors in PSaC, despite the absence of structural damage on CT imaging. Whereas the anterior thalamus and dorsomedial thalamus have been previously associated with the salience network, Kawabata et al.⁸¹

found that the ventral anterior and ventral lateral thalamus exhibited the strongest connections with salience/cingulo-opercular networks. In addition, changes in salience network connectivity over time appear to be associated with symptom recovery following mTBI^{51,82}. Given the diverse symptomatology associated with salience network dysfunction in PSaC, it prompts further investigation into the network's role in symptom generation and persistence.

On the basis of included studies employing a seed-based connectivity approach, PSaC+ studies were found to have selectively increased functional connectivity between bilateral DLPFC and multiple salience network nodes compared with PSaC-, including the right insula, right amygdala/putamen, supplementary motor cortex and left supramarginal gyrus^{26,27,38,39}. These regions have been linked to neuropsychological factors commonly observed in PSaC, including altered interoceptive awareness⁸³, heightened sensory sensitivity²¹ and diminished cognitive control, respectively⁸⁴. By contrast, reduced functional connectivity was found between the right DLPFC and left midbrain (salience network)⁴⁴, as well as right supramarginal gyrus (salience network) and bilateral posterior parietal cortex (executive-control network), potentially reflecting diminished top-down regulation of sensory and attentional systems^{27,85}. For salience network–dorsal attention network connectivity, increased connectivity was observed between the right supramarginal gyrus and the right superior parietal lobule (areas involved in working memory and attentional control) and the multisensory processing area of the temporoparietal junction^{40,47}. In addition to changes in the salience network being discovered in significantly more PSaC+ studies than PSaC- studies ($P = 0.026$), these findings highlight a unique connectivity profile that further characterizes individuals with PSaC. These patterns include features linked to symptom preoccupation and hypervigilance, which are core to somatization, a factor strongly associated with salience network dysfunction and risk of developing PSaC^{9,72}.

PSaC+ and PSaC- studies were not differentiated by the degree of salience network–default-mode network connectivity (Supplementary Table 7), but this network pairing represented the majority of extracted coordinates from seed-based and ROI-ROI functional connectivity studies (33%) and was the most commonly investigated network *a priori* across included studies (Supplementary Table 2). Among the PSaC+ studies, reduced anticorrelation between the default-mode network and the salience network (including bilateral insula, left premotor cortex and bilateral supramarginal gyrus) was identified^{39,40}. Interactions between salience network–default-mode network on inefficient cognitive control in patients with cognitive impairment following TBI have been previously reported by Bonnelle et al.²² However, default-mode network changes in PSaC have not been consistently found^{23,27,42,44}. More recently, Trapp et al.⁸⁶ conducted a large-scale investigation examining the relationship between penetrative TBI in veterans and persistent depressive symptoms, revealing that damaged regions within the salience network, such as the bilateral anterior insula and dorsolateral prefrontal cortex, were identified as ‘risk’ regions associated with higher depression severity. Conversely, structurally damaged regions within the default-mode network, including the right orbitofrontal cortex and medial prefrontal cortex, were identified as ‘resilience’ regions associated with lower depression severity. It is interesting to note that our network meta-analysis revealed greater default-mode network, but not salience network, activation in PSaC- studies, whereas PSaC+ studies revealed the opposite.

Regarding the coordinate-based ALE analysis, the lack of statistically significant spatial clustering is not in line with previous findings^{87,88}. Importantly, these studies included task-based fMRI, whereas our study included only resting-state fMRI results. In addition, our meta-analysis of resting-state fMRI whole-brain studies was probably underpowered to detect significant effects. The number of studies meeting criteria for ALE ($n = 7$) was below the recommended range of experiments ($n = 17$ –20) to yield adequate statistical power

in simulations⁸⁹. Lack of statistically significant spatial clustering could also have been due to heterogeneity between studies in terms of demographics (sex, age, comorbidities, veteran versus civilian versus athlete), clinical characteristics (time from injury to scan, degree of symptomatology) and fMRI procedures (statistical thresholding/correction, ROI selection, resting-state method use (seed-based analysis versus independent component analysis versus ROI-ROI); (Table 1 and Supplementary Table 2)). However, unthresholded ALE maps revealed a pattern of disruption with notable localization to the salience network. Thus, despite these factors, multiple lines of analysis in our study have convergent findings in the salience network.

Other notable network changes outside the salience network in PSaC+ studies include the somatomotor and visual networks, both of which were found to have increased connectivity with all networks and distinguished PSaC+ and PSaC- studies (Fig. 2c). Given the presence of visual, vestibular and pain symptoms commonly reported in PSaC, it is not surprising to see hyperconnectivity and hyperactivation among these networks^{40,42,90}. The visual network was also found to have considerable activation across binarized z-map thresholds in the network-based meta-analytic approach of PSaC+ studies, which was not found across PSaC- studies (Fig. 3).

The DLPFC has been most commonly targeted in PSaC, although targeting has relied on scalp-based heuristics²⁸. Our study may help inform DLPFC targets for PSaC. To this end, we derived network maps using two separate approaches: we derived (1) a whole-brain functional connectivity map from the anterior insula cluster identified in the symptom-based network analysis using Neurosynth data and (2) a coordinate-based network utilizing all previously reported activation/deactivation coordinates from resting-state functional connectivity studies examining those with PSaC+ compared with PSaC- following concussion/mTBI. Both approaches converged to implicate the salience network (Figs. 2 and 3 and Supplementary Fig. 3). Our Neurosynth seed-to-voxel connectivity analysis using the bilateral anterior insula as a seed region demonstrated regions of both positive and negative functional connectivity across the DLPFC and anticorrelated with regions of the default-mode network, such as the medial prefrontal cortex and angular gyrus (Fig. 4). Notably, while the DLPFC is a common stimulation target in depression, it is a heterogeneous region with functionally distinct subregions⁹¹. The DLPFC target identified in our PSaC analysis localized more medially compared with the typical lateral DLPFC region targeted using Beam F3 in depression protocols (Fig. 4)⁹². This distinction may reflect the broader symptom profile of PSaC, which extends beyond mood symptoms to include cognitive, sensory and somatic complaints. The PSaC-linked circuit identified here therefore maps onto a wider constellation of symptoms than dysphoria alone.

The seed-based connectivity map generated from the bilateral anterior insula/salience network cluster identified from the Neurosynth analysis demonstrated close agreement with the coordinate-based network map, as indicated in the convergence map (Fig. 4). Regions where there was no convergence were typically areas of weak functional connectivity in the Neurosynth map and low z scores in the coordinate-based network map (that is, areas that were already not strongly implicated in either analysis). These analyses indicated two broad regions of maximal convergence in the prefrontal cortex, implicating potential brain stimulation targets of positive and negative functional connectivity. The most clinically effective combination of target region and TMS frequency will require further investigation. Cortical sites of both negative and positive connectivity to downstream regions have been implicated in clinical response^{93,94}. A further consideration is that it remains uncertain whether these distinct DLPFC regions represent a causal or compensatory network in PSaC, and whether stimulating these areas would prove beneficial or potentially deleterious to the recovery process.

Finally, a major goal has been to personalize care in PSaC, a challenge due to its heterogeneity^{4,5}. The identification of a core network

of dysfunction accessible by personalized rTMS offers a therapy that can potentially be used across PSaC presentations. The application of individualized resting-state network mapping has demonstrated improved accuracy of stimulation protocols for TBI-related depression, potentially enhancing TMS treatment efficacy^{15,35}. However, robust clinical data utilizing this approach on outcomes in PSaC/TBI-related depression are lacking. Moreover, it is worth noting that TBI-associated depression has been characterized primarily by increased connectivity between the default-mode network and dorsal attention network, as well as enhanced connectivity between the dorsal attention network and the subgenual anterior cingulate cortex⁹⁵. The dorsal attention network was found to be disrupted in almost 80% of included PSaC+ studies (versus 57% in the PSaC- group), although this difference was not statistically significant. Our network-based meta-analysis of coordinates from studies using whole-brain connectivity did not find spatial overlap with the dorsal attention network in either PSaC+ or PSaC- studies. This discrepancy may speak to the heterogeneity and complexity in considering the broader PSaC category, as opposed to more selective phenotyping of post-TBI depression. Of note, the study by Siddiqui et al.⁹⁵ included samples of more severe TBI than concussion, which may also account for the discrepancy. Overall, given the lack of effective treatments and early stage of neuromodulation approaches for TBI, new network targets that may be aligned with the underlying pathophysiology of PSaC are needed to guide future treatment trials.

Limitations

There are many limitations that need to be highlighted. First, the RPQ symptom-activation maps derived from Neurosynth meta-analytic data involved task-based fMRI studies with non-TBI participants, and the findings could be confounded by comorbidities unrelated to PSaC. Meta-analytic data were not available for several RPQ symptom domains (nausea/vomiting, dizziness/imbalance, blurred/double vision and processing speed). It is possible that the union of multiple task-based fMRI studies, regardless of condition, could involve salience network activation as a common feature⁶⁶. However, incorporating a concussion-specific meta-analytic activation map derived using Neurosynth Compose and filtered to include only concussion studies yielded stable results when combined with the RPQ symptom-activation map, reinforcing the association between PSaC symptoms and salience network topology. Disruption of a pivotal hub that coordinates diverse functions across domains emphasizes the role of the salience network in understanding the various symptoms in PSaC.

Second, our network mapping approach was limited to studies that reported coordinates. Within the studies included in our systematic review, there was substantial heterogeneity in the categorization, diagnosis and neuroimaging evaluation of PSaC. For example, there were proportionally more longitudinal prospective studies in the PSaC- group of studies, which may have a lower likelihood of capturing high-symptom PSaC over time as compared with cross-sectional studies focusing on high-symptom PSaC, which would introduce bias in our results. Regarding control groups, PSaC+ studies primarily used healthy controls, whereas PSaC- studies predominantly used a prospective design with comparisons between acute injury and follow-up assessments, often without a healthy/non-TBI control group. Although our intention was to include studies that classified patients as recovered or having low symptom burden, it is possible that some individuals in these groups were still recovering or experiencing residual PSaC symptoms. This variability in symptom severity and recovery stage among patients may have introduced confounding factors that influenced resting-state functional connectivity results.

In addition, there were relatively fewer low-symptom/recovery studies, and only three that used whole-brain analysis, which precluded ALE meta-analysis for PSaC-, thus limiting comparisons with PSaC+ studies. Notably, half of the MNI coordinates that mapped to the salience network across PSaC- studies were derived from a single

study⁵⁴, whereas for the PSaC+ studies the highest contribution from a single study was 15% (ref. 26). However, this observation further highlights the convergent evidence across studies linking the salience network to PSaC+. The results of the network-based meta-analysis are limited by the relatively low number of studies using non-seed-based whole-brain connectivity approaches. Among the PSaC+ studies, 60 coordinates from 5 studies were used, whereas for PSaC- studies, only 9 coordinates from 3 studies could be used. This imbalance may reflect a combination of factors, including our stringent inclusion criteria (for example, resting-state fMRI data collected at least 1 month post-injury, extractable activation coordinates), the availability of usable data for analysis, or broader trends in the neuroimaging literature that emphasize studies of persistent symptoms²⁰.

While our study included individuals with chronic persisting symptoms irrespective of mechanism of injury, we acknowledge that blast-related mTBI may differ from sports-related concussion in terms of symptomatology and psychiatric risk factors^{96,97}. However, the proportion of coordinates from veteran populations was relatively balanced between PSaC+ and PSaC- studies, and the included studies did not focus exclusively on blast-related injuries. Thus, while these differences should be considered in the interpretation of findings, we do not believe they bias the results.

Last, regarding potential therapeutic target sites, the incongruity between the seed-based connectivity map and network meta-analysis raises critical questions about the functional importance of these discrepant DLPFC areas in the context of PSaC. Specifically, it remains unclear whether these discrepant areas within the DLPFC represent a causal or compensatory network in PSaC. In addition, the potential consequences of stimulating these areas on the clinical recovery of PSaC patients remain to be explored. Future studies are recommended to include a retrospective validation or lesion-based network approach.

Conclusions

Our study sought to explore the core neural underpinnings of persisting symptoms after concussion (PSaC) to identify a canonical network potentially suitable for targeted neuromodulation therapies. Our findings underscore the salience network as a neural hub that is disproportionately affected in PSaC across multiple analytic approaches, serving as an anchor for core PSaC symptoms. Personalized network mapping using data from the Human Connectome Project identified an area of the DLPFC maximally co-activated/correlated with the salience network as a candidate target for tailored brain stimulation interventions. It is essential to interpret these results cautiously due to limitations in symptom-activation map generation, availability of data in published literature, heterogeneity across included studies and lack of retrospective validation. Nevertheless, the consistent emergence of the salience network in PSaC+ studies underscores its pivotal role in chronic symptoms following concussion/mTBI, offering promise for the development of targeted therapeutic interventions in PSaC within the evolving field of brain stimulation.

Methods

PSaC symptom-based network mapping

To identify a functional network that is clinically pertinent to PSaC, we used the Neurosynth database (<http://www.neurosynth.org>) to extract meta-analytic activation maps from search terms approximated to symptoms on the 16-item RPQ. The RPQ is a diagnostic tool commonly used to diagnose PSaC and includes somatic, affective, cognitive and behavioral components, with higher scores reflecting higher symptom burden^{50,98}. The homologous RPQ search terms were identified in the Neurosynth database (Fig. 2a) and included ‘anxiety’, ‘depressive disorders’, ‘visual stimuli’, ‘auditory stimuli’, ‘impulsivity’, ‘angry’, ‘memory’, ‘concentration’, ‘pain’, ‘sleep’ and ‘arousal’. The Neurosynth database contains 14,371 whole-brain human fMRI studies and automatically computes Pearson correlation coefficients between

submitted whole-brain maps and 1,334 terms used in contributed publications. Neurosynth computes these activation maps by performing meta-analyses across thousands of whole-brain fMRI studies using a uniformity test (a one-way analysis of variance) to identify voxels that are consistently reported as active in studies using a given term. These maps represent the spatial distribution of activation consistently associated with each term and are publicly available for download. Each activation map was binarized in FSLeyes (Functional Magnetic Resonance Imaging of the Brain (FMRIB) Software Library (FSL), version 1.6.1, 2023)⁹⁹ by assigning a value of 1 to all voxels with nonzero z -scores, and 0 otherwise, to reflect the spatial extent of consistent activation associated with each term. The union of these binarized maps was then used to compute common regions of functional activation across approximated RPQ symptom–term domains.

These neuroimaging studies did not include primarily patients with mTBI (Supplementary Table 8). To further refine the symptom-based network map with data from a more clinically specific population, we conducted a targeted meta-analysis using Neurosynth Compose, a new tool that allows for study-level filtering. We selected 37 studies explicitly involving participants with concussion, yielding a total of 57 contrasts and 847 reported MNI coordinates. We conducted a coordinate-based meta-analysis using the MKDAChi² algorithm with the following parameters: kernel radius of 10 mm, kernel value of 1 and prior probability of 0.5. Multiple comparisons correction was performed using a false discovery rate corrector ($\alpha = 0.05$, independent method). The resulting z -score activation map was binarized using FSLeyes and overlaid with the union of all RPQ symptom–activation maps. The full meta-analysis output is publicly available¹⁰⁰.

Systematic review of PSaC resting-state-based network mapping

To investigate whether our RPQ symptom map co-localized to PSaC network dysfunction reported in the literature, we conducted a systematic review of PubMed and MEDLINE databases for all studies published between January 2000 and September 2023 that examined resting-state fMRI in mTBI or concussion. We also searched reference lists of reviewed papers to identify other relevant papers. Studies were categorized into PSaC+ or PSaC– focused. To differentiate between high and low symptom burden in PSaC studies, we classified studies on the basis of their primary clinical outcome measures at the time of neuroimaging. Studies that explicitly diagnosed PCS using standardized criteria (for example, ICD-10 or DSM-IV) and/or applied predefined cut-off scores for symptom severity (for example, RPQ > 30, HAM-D > 8, CAPS > 2) or categorical distinctions (for example, absent/mild versus severe on a rating scale) were classified accordingly. When no clear cut-off was provided, we determined symptom burden grouping by assessing whether reported scores on primary clinical outcomes exceeded (PSaC+ studies) or fell below (PSaC– studies) recognized thresholds associated with greater symptom severity and poor recovery. These classifications were systematically applied across all included studies (Supplementary Table 4). The rationale for diagnosing PSaC on the basis of >1 month of persistent symptoms was supported by several studies^{3,27}.

Articles were reviewed for inclusion by two independent researchers (A.M. and I.J.S.), and discrepancies were resolved by S.M.N. This systematic review followed PRISMA guidelines (see PRISMA checklist in Supplementary Methods for further detail). We included articles that (1) contained original, peer-reviewed research, (2) involved adult participants and (3) collected resting-state fMRI data at least 1 month following mTBI. Data extraction, including clinical, methodological and demographic variables, was completed by two investigators (A.M. and C.F.D.L.). Quality assessment of the included studies was conducted by two investigators (A.M. and C.F.D.L.) using the quality assessment tools for Observational Cohort and Cross-Sectional Studies and Controlled Intervention Studies¹⁰¹.

Statistical analysis of coordinates derived from systematic review

To assess network differences associated with persistent symptoms, we compared the distribution of activation coordinates from PSaC+ versus PSaC– studies by mapping their reported peak coordinates onto canonical large-scale brain networks using FSLeyes (version 1.6.1, 2023). In addition, two studies directly compared high versus low symptom burden PSaC groups and were categorized accordingly (Supplementary Table 2).

For each study, we extracted peak activation coordinates of regions showing statistically significant between-group differences with controls. Talairach coordinates were converted to MNI space using GingerALE’s Talairach-to-MNI conversion tool (<http://brainmap.org/ale/>)^{102,103}. To determine affected networks, all peak MNI coordinates derived from the systematic review were overlaid on the Yeo 2011 7-network atlas and Yeo/Schaefer 2018 17-network atlas using Schaefer 400- and 1,000-parcel resolutions in FSLeyes^{63,104}. Each coordinate was assigned a value of 1 for a single-network assignment or 0.5 if it spatially overlapped two adjacent networks. This approach allowed for equal representation of coordinates near network boundaries. While activations and deactivations were documented separately for descriptive purposes, the same mapping and scoring procedure was applied to both. The full list of MNI coordinates extracted during systematic review is publicly available¹⁰⁵.

This mapping allowed us to estimate the distribution of activation and deactivation peaks across large-scale brain networks. To enable group-level comparisons, we then binarized network involvement at the study level: if a given network contained at least one assigned coordinate (1 or 0.5), it was coded as ‘1’ (altered) for that study; otherwise, it was coded as ‘0’ (unaffected). This allowed us to perform a Fisher’s exact test comparing the frequency of network involvement between PSaC+ and PSaC– studies. A similar methodology was employed in ref. 106. Analyses were performed in SPSS (version 29, IBM Corp.)¹⁰⁷.

Coordinate-based meta-analysis of network stability

To evaluate whether there was statistically significant spatial clustering of coordinates across PSaC+ studies, we performed a coordinate-based meta-analysis using ALE. This method identifies regions where reported activation peaks from different studies converge spatially more than would be expected by chance, highlighting localized effects. While this identifies potential regional spatial convergence, it does not directly assess the broader network-level connectivity patterns associated with these coordinates. The ALE method was implemented via GingerALE (version 3.0.2; <http://brainmap.org/ale/>). This method has been previously described¹⁰⁸. All analyses were performed in MNI space, accounting for multiple comparisons with a cluster-forming threshold of $P < 0.001$ (uncorrected) and a cluster-level family-wise error rate of 5% (ref. 109). Given the limited number of PSaC– studies, this analysis was performed on PSaC+ studies that used a seed-based, whole-brain voxel approach with default-mode network or executive-control network as the seed network. The goal was to determine whether any significant activation clusters emerged and, if so, to identify the associated network. Studies using ROI-to-ROI connectivity (that is, non-whole-brain analyses) were excluded from ALE analysis.

Network-based meta-analysis of network stability

Another approach to determining which network the coordinates derived from the systematic review predominantly mapped onto involved a network-based meta-analytic approach. Unlike ALE, which relies on the spatial convergence of activation clusters, this method assesses which functional networks are preferentially involved by examining the distribution of coordinates across the whole brain and their connectivity patterns within a large normative dataset.

As an overview, coordinates were derived as described in the preceding, but only experiments utilizing whole-brain group analyses

were included; those utilizing ROI seed-based analyses were excluded (see Supplementary Table 2 for details on which studies employed whole-brain analysis and where coordinates were derived from). Next, whole-brain functional connectivity was computed for each coordinate using resting-state fMRI images from 100 healthy adults participating in the HCP^{110,111}. These networks were summed and divided by the total number of constituent coordinates to generate a mean functional connectivity map. PSaC+ and PSaC– functional connectivity maps were then subjected to statistical testing against a null distribution and converted to z-scored brain maps (Supplementary Fig. 3)¹¹².

We analyzed data from the first two fMRI sessions in the HCP database, acquired consecutively on the first day of scanning. Each of the two data acquisition sessions comprised 14 min, 33 s runs (right-to-left and left-to-right phase encodings, 1,200 volumes each), with eyes open and relaxed fixation on a projected bright crosshairs on a dark background (and presented in a darkened room). These two 14 min, 33 s runs per day were temporally concatenated (following preprocessing, described next) to result in 29 min of data and 2,400 datapoints per concatenated scan. To minimize temporal discontinuity, the mean was removed from each time series before concatenation. For additional details regarding concatenation and the HCP functional preprocessing pipeline, see Supplementary Methods section Network-based meta-analysis.

Spherical seeds (4 mm radius) were centered at each reported coordinate. Whole-brain functional connectivity maps were then computed by correlating the mean time series from this sphere with time series for every voxel composing a gray-matter mask (FSL MNI 152 2 mm brain template). The functional connectivity maps from all coordinates in a given condition (that is, PSaC+ and PSaC–) were summed voxel-wise, and the summand was divided by the total number of constituent coordinates to generate a condition-specific functional connectivity map. This procedure was repeated for 100 individuals, and the resulting functional connectivity maps were averaged to generate a single normative functional connectivity map for each condition.

Next, the mean functional connectivity map for each condition (PSaC+ and PSaC–) was subjected to statistical testing. This procedure mimicked that described in the preceding except that functional connectivity maps were derived from randomly generated (rather than real) coordinates uniformly distributed throughout the gray-matter volume. The same sample of 100 individuals from the HCP was used to compute functional connectivity maps. For a given condition, the number of contributing coordinates (*n* coordinates) was also held identical across observed (real) and randomly generated (null) functional connectivity maps. This procedure was repeated 1,000 times per condition to generate 1,000 group-average functional connectivity maps, each derived from *n* coordinates. We used this empirical null distribution to test the alternative hypothesis that the observed coordinates were constrained to specific functional networks. To this end, a z-score map was computed by subtracting the mean of the 1,000 null samples from the observed functional connectivity map and dividing the result by the standard deviation across the 1,000 null samples. This was performed independently for each gray-matter voxel and condition, yielding a z-score map for each condition. These z-scored condition-specific brain network maps are referred to as ‘brain maps’. In simpler terms, these brain maps provide a representation of the connectivity of dysfunctional brain regions in individuals with TBI presenting with (PSaC+) or without (PSaC–) PSaC, and every voxel value corresponds to the level of deviation from what would be expected by chance (as defined by the null distribution).

To understand the etiology of the brain maps derived, we next computed spatial alignment with canonical (Yeo-7) functional networks (Supplementary Fig. 3). The Dice correlation coefficient was utilized for this purpose as it allows computation of spatial similarity with a binarized network (that is, with Yeo networks). Given that the arbitrarily

selected threshold necessary to binarize PSaC+ and PSaC– networks might influence spatial correlations, this computation was performed with absolute z maps thresholded at 10, 15, 20, 25 and 30% increments (Supplementary Fig. 3). The mean spatial correlation was computed across these thresholds.

Deriving neuromodulation targets for PSaC

Last, to determine whether a cortical target for neuromodulation could be identified within the network implicated in PSaC, we examined the functional connectivity of the key regions identified in the previous analyses. This approach aimed to establish a site within the affected network that could serve as a potential intervention target on the basis of its connectivity profile and convergence across multiple mapping methods.

A functional connectivity map was derived from the two bilateral anterior insula clusters identified in the preceding in the Neurosynth symptom-mapping step using minimally preprocessed data from the HCP ($N = 1,000$ concatenated 28-min resting-state fMRI scans) and previously detailed methods^{111,113}. This involved (1) deriving the mean time series across both clusters for each participant; (2) computing a whole-brain functional connectivity map for each participant; and (3) generating a group-average functional connectivity map. We computed the convergence of this map with the coordinate-based network brain map generated from PSaC+ coordinates derived above from our systematic review (Supplementary Fig. 4). The convergence map was created by voxel-wise multiplication of Neurosynth-derived seed-based and coordinate-based network meta-analytic maps, such that when the product of multiplication is positive it demonstrates convergence.

Reporting summary

Further information on research design is available in the Nature Portfolio Reporting Summary linked to this article.

Data availability

The full meta-analytic output from the Neurosynth Compose analysis is publicly available at <https://identifiers.org/neurovault.collection:20829> (ref. 100) The dataset supporting the findings of this study (that is, the full list of MNI coordinates extracted during the systematic review) is publicly available at https://osf.io/dpzmy/?view_only=4e9a8c0d37c464f98ba8cc7521a43d7 (ref. 105).

References

1. Voormolen, D. C. et al. Divergent classification methods of post-concussion syndrome after mild traumatic brain injury: prevalence rates, risk factors, and functional outcome. *J. Neurotrauma* **35**, 1233–1241 (2018).
2. Broshek, D. K., Pardini, J. E. & Herring, S. A. Persisting symptoms after concussion: time for a paradigm shift. *PM R* **14**, 1509–1513 (2022).
3. Tator, C. H. & Davis, H. The postconcussion syndrome in sports and recreation: clinical features and demography in 138 athletes. *Neurosurgery* **75**, S106–S112 (2014).
4. Clark, C. N. et al. Reframing postconcussion syndrome as an interface disorder of neurology, psychiatry and psychology. *Brain* **145**, 1906–1915 (2022).
5. Mollica, A., Dey, A., Cairncross, M., Silverberg, N. & Burke, M. J. Neuropsychiatric treatment for mild traumatic brain injury: nonpharmacological approaches. *Semin. Neurol.* **42**, 168–181 (2022).
6. Silverberg, N. D. et al. Management of concussion and mild traumatic brain injury: a synthesis of practice guidelines. *Arch. Phys. Med. Rehabil.* **101**, 382–393 (2020).
7. Broshek, D. K., De Marco, A. P. & Freeman, J. R. A review of post-concussion syndrome and psychological factors associated with concussion. *Brain Inj.* **29**, 228–237 (2015).

8. Picon, E. L. et al. Factors perpetuating functional cognitive symptoms after mild traumatic brain injury. *J. Clin. Exp. Neuropsychol.* **45**, 988–1002 (2023).
9. Nelson, L. D. et al. Preinjury somatization symptoms contribute to clinical recovery after sport-related concussion. *Neurology* **86**, 1856–1863 (2016).
10. Theadom, A. et al. Persistent problems 1 year after mild traumatic brain injury: a longitudinal population study in New Zealand. *Br. J. Gen. Pract.* **66**, e16–e23 (2016).
11. Iverson, G. L. et al. Predictors of clinical recovery from concussion: a systematic review. *Br. J. Sports Med.* **51**, 941–948 (2017).
12. Gumus, M. et al. Brain connectivity changes in postconcussion syndrome as the neural substrate of a heterogeneous syndrome. *Brain Connect.* **12**, 711–724 (2022).
13. Van Der Horn, H. J. et al. The default mode network as a biomarker of persistent complaints after mild traumatic brain injury: a longitudinal functional magnetic resonance imaging study. *J. Neurotrauma* **34**, 3262–3269 (2017).
14. Woodrow, R. E. et al. Acute thalamic connectivity precedes chronic post-concussive symptoms in mild traumatic brain injury. *Brain* **146**, 3484–3499 (2023).
15. Siddiqi, S. H. et al. Individualized precision targeting of dorsal attention and default mode networks with rTMS in traumatic brain injury-associated depression. *Sci. Rep.* **13**, 4052 (2023).
16. Mollica, A., Greben, R., Oriuwa, C., Siddiqi, S. H. & Burke, M. J. Neuromodulation treatments for mild traumatic brain injury and post-concussive symptoms. *Curr. Neurol. Neurosci. Rep.* **22**, 171–181 (2022).
17. Shi, S., Picon, E. L., Rioux, M., Panenka, W. J. & Silverberg, N. D. Catastrophizing is associated with excess cognitive symptom reporting after mild traumatic brain injury. *Neuropsychology* **38**, 126–133 (2024).
18. Silverberg, N. D., Panenka, W. J. & Iverson, G. L. Fear avoidance and clinical outcomes from mild traumatic brain injury. *J. Neurotrauma* **35**, 1864–1873 (2018).
19. Buzzanca-Fried, K. E. et al. Psychological constructs from the fear avoidance model and beyond as predictors for persisting symptoms after concussion: an integrative review. *Arch. Phys. Med. Rehabil.* **105**, 2362–2374 (2024).
20. Gumus, M., Santos, A. & Tartaglia, M. C. Diffusion and functional MRI findings and their relationship to behaviour in postconcussion syndrome: a scoping review. *J. Neurol. Neurosurg. Psychiatry* **92**, 1259–1270 (2021).
21. Hoffman, A. N., Lam, J., Hovda, D. A., Giza, C. C. & Fanselow, M. S. Sensory sensitivity as a link between concussive traumatic brain injury and PTSD. *Sci. Rep.* **9**, 13841 (2019).
22. Bonnelle, V. et al. Salience network integrity predicts default mode network function after traumatic brain injury. *Proc. Natl Acad. Sci. USA* **109**, 4690–4695 (2012).
23. Van Der Horn, H. J., Liemburg, E. J., Aleman, A., Spikman, J. M. & Van Der Naalt, J. Brain networks subserving emotion regulation and adaptation after mild traumatic brain injury. *J. Neurotrauma* **33**, 1–9 (2016).
24. Messé, A. et al. Specific and evolving resting-state network alterations in post-concussion syndrome following mild traumatic brain injury. *PLoS ONE* **8**, e65470 (2013).
25. Li, X. et al. Brain dynamics in triple-network interactions and its relation to multiple cognitive impairments in mild traumatic brain injury. *Cereb. Cortex* **33**, 6620–6632 (2023).
26. Wong, J. K. Y., Churchill, N. W., Graham, S. J., Baker, A. J. & Schweizer, T. A. Altered connectivity of default mode and executive control networks among female patients with persistent post-concussion symptoms. *Brain Inj.* **37**, 147–158 (2023).
27. Shafi, R. et al. Sex-specific differences in resting-state functional connectivity of large-scale networks in postconcussion syndrome. *Sci. Rep.* **10**, 21982 (2020).
28. Mollica, A. et al. Transcranial magnetic stimulation for the treatment of concussion: a systematic review. *Neuromodulation* **24**, 803–812 (2021).
29. Tsai, P.-Y., Chen, Y.-C., Wang, J.-Y., Chung, K.-H. & Lai, C.-H. Effect of repetitive transcranial magnetic stimulation on depression and cognition in individuals with traumatic brain injury: a systematic review and meta-analysis. *Sci. Rep.* **11**, 16940 (2021).
30. Koski, L. et al. Noninvasive brain stimulation for persistent postconcussion symptoms in mild traumatic brain injury. *J. Neurotrauma* **32**, 38–44 (2015).
31. Moussavi, Z. et al. A pilot randomised double-blind study of the tolerability and efficacy of repetitive transcranial magnetic stimulation on persistent post-concussion syndrome. *Sci. Rep.* **9**, 5498 (2019).
32. Brunoni, A. R. et al. Repetitive transcranial magnetic stimulation for the acute treatment of major depressive episodes: a systematic review with network meta-analysis. *JAMA Psychiatry* **74**, 143–152 (2017).
33. Lambert, M. et al. Depressive symptoms in individuals with persistent postconcussion symptoms: a systematic review and meta-analysis. *JAMA Netw. Open* **5**, e2248453 (2022).
34. Doroszkiewicz, C. et al. Anxiety, depression, and quality of life: a long-term follow-up study of patients with persisting concussion symptoms. *J. Neurotrauma* **38**, 493–505 (2021).
35. Siddiqi, S. H. et al. Repetitive transcranial magnetic stimulation with resting-state network targeting for treatment-resistant depression in traumatic brain injury: a randomized, controlled, double-blinded pilot study. *J. Neurotrauma* **36**, 1361–1374 (2019).
36. Ning, L., Makris, N., Camprodon, J. A. & Rathi, Y. Limits and reproducibility of resting-state functional MRI definition of DLPFC targets for neuromodulation. *Brain Stimul.* **12**, 129–138 (2019).
37. Dumkrieger, G., Chong, C. D., Ross, K., Berisha, V. & Schwedt, T. J. Static and dynamic functional connectivity differences between migraine and persistent post-traumatic headache: a resting-state magnetic resonance imaging study. *Cephalgia* **39**, 1366–1381 (2019).
38. Vedaei, F. et al. Resting-state functional MRI metrics in patients with chronic mild traumatic brain injury and their association with clinical cognitive performance. *Front. Hum. Neurosci.* **15**, 768485 (2021).
39. Sours, C. et al. Default mode network interference in mild traumatic brain injury—a pilot resting state study. *Brain Res.* **1537**, 201–215 (2013).
40. Amir, J. et al. Atypical resting state functional connectivity in mild traumatic brain injury. *Brain Behav.* **11**, e2261 (2021).
41. Leung, A. et al. Diminished supraspinal pain modulation in patients with mild traumatic brain injury. *Mol. Pain* **12**, 1744806916662661 (2016).
42. Rockswold, S. B. et al. Functional magnetic resonance imaging and oculomotor dysfunction in mild traumatic brain injury. *J. Neurotrauma* **36**, 1099–1105 (2019).
43. Sheth, C., Rogowska, J., Legarreta, M., McGlade, E. & Yurgelun-Todd, D. Functional connectivity of the anterior cingulate cortex in veterans with mild traumatic brain injury. *Behav. Brain Res.* **396**, 112882 (2021).
44. Runyan, A. et al. Comparing resting-state connectivity of working memory networks in US Service members with mild traumatic brain injury and posttraumatic stress disorder. *Brain Res.* **1796**, 148099 (2022).

45. Sours, C., Zhuo, J., Roys, S., Shanmuganathan, K. & Gullapalli, R. P. Disruptions in resting state functional connectivity and cerebral blood flow in mild traumatic brain injury patients. *PLoS ONE* **10**, e0134019 (2015).
46. Stevens, M. C. et al. Multiple resting state network functional connectivity abnormalities in mild traumatic brain injury. *Brain Imaging Behav.* **6**, 293–318 (2012).
47. Trofimova, A. et al. Alterations in resting-state functional brain connectivity and correlations with vestibular/ocular-motor screening measures in postconcussion vestibular dysfunction. *J. Neuroimaging* **31**, 277–286 (2021).
48. D’Souza, M. M. et al. Alterations of connectivity patterns in functional brain networks in patients with mild traumatic brain injury: a longitudinal resting-state functional magnetic resonance imaging study. *Neuroradiol. J.* **33**, 186–197 (2020).
49. Ingebrigtsen, T., Waterloo, K., Marup-Jensen, S., Attner, E. & Romner, B. Quantification of post-concussion symptoms 3months after minor head injury in 100 consecutive patients. *J. Neurol.* **245**, 609–612 (1998).
50. Zeldovich, M. et al. Reference values for the Rivermead Post-Concussion Symptoms Questionnaire (RPQ) from general population samples in the United Kingdom, Italy, and the Netherlands. *J. Clin. Med.* **11**, 4658 (2022).
51. Chong, C. D., Wang, L., Wang, K., Traub, S. & Li, J. Homotopic region connectivity during concussion recovery: a longitudinal fMRI study. *PLoS ONE* **14**, e0221892 (2019).
52. Churchill, N. W., Hutchison, M. G., Graham, S. J. & Schweizer, T. A. Mapping brain recovery after concussion: from acute injury to 1 year after medical clearance. *Neurology* **93**, e1980–e1992 (2019).
53. De Souza, N. L., Parker, R., Gonzalez, C. S., Ryan, J. D. & Esopenko, C. Effect of age at time of injury on long-term changes in intrinsic functional connectivity in traumatic brain injury. *Brain Inj.* **34**, 1646–1654 (2020).
54. McCuddy, W. T. et al. Association of acute depressive symptoms and functional connectivity of emotional processing regions following sport-related concussion. *Neuroimage Clin.* **19**, 434–442 (2018).
55. Chin, E. Y., Nelson, L. D., Barr, W. B., McCrory, P. & McCrea, M. A. Reliability and validity of the Sport Concussion Assessment Tool-3 (SCAT3) in high school and collegiate athletes. *Am. J. Sports Med.* **44**, 2276–2285 (2016).
56. Downey, R. I., Hutchison, M. G. & Comper, P. Determining sensitivity and specificity of the Sport Concussion Assessment Tool 3 (SCAT3) components in university athletes. *Brain Inj.* **32**, 1345–1352 (2018).
57. Mitra, B. et al. Long-term outcomes of major trauma patients with concussion. *Injury* **54**, 75–81 (2023).
58. Zimmerman, M., Martinez, J. H., Young, D., Chelminski, I. & Dalrymple, K. Severity classification on the Hamilton Depression Rating scale. *J. Affect. Disord.* **150**, 384–388 (2013).
59. Flowers, M. et al. Severities in persistent mild traumatic brain injury related headache is associated with changes in supraspinal pain modulatory functions. *Mol. Pain* **17**, 17448069211037881 (2021).
60. Seeley, W. W. et al. Dissociable intrinsic connectivity networks for salience processing and executive control. *J. Neurosci.* **27**, 2349–2356 (2007).
61. Menon, V. in *Brain Mapping: An Encyclopedic Reference* Vol. 2 (ed. Toga, A.) 597–611 (Academic, Elsevier 2015).
62. Dosenbach, N. U. F. et al. Distinct brain networks for adaptive and stable task control in humans. *Proc. Natl Acad. Sci. USA* **104**, 11073–11078 (2007).
63. Thomas et al. The organization of the human cerebral cortex estimated by intrinsic functional connectivity. *J. Neurophysiol.* **106**, 1125–1165 (2011).
64. Uddin, L. Q., Yeo, B. T. T. & Spreng, R. N. Towards a universal taxonomy of macro-scale functional human brain networks. *Brain Topogr.* **32**, 926–942 (2019).
65. Downar, J., Blumberger, D. M. & Daskalakis, Z. J. The neural crossroads of psychiatric illness: an emerging target for brain stimulation. *Trends Cogn. Sci.* **20**, 107–120 (2016).
66. Menon, V. & Uddin, L. Q. Saliency, switching, attention and control: a network model of insula function. *Brain Struct. Funct.* **214**, 655–667 (2010).
67. Seeley, W. W. The salience network: a neural system for perceiving and responding to homeostatic demands. *J. Neurosci.* **39**, 9878–9882 (2019).
68. Goodkind, M. et al. Identification of a common neurobiological substrate for mental illness. *JAMA Psychiatry* **72**, 305–315 (2015).
69. Taylor, J. J. et al. A transdiagnostic network for psychiatric illness derived from atrophy and lesions. *Nat. Hum. Behav.* **7**, 420–429 (2023).
70. Raji, T. T. et al. Depression core network-based individualized targeting for transcranial magnetic stimulation. *Brain Stimul.* **16**, 619–627 (2023).
71. Mitra, A., Raichle, M. E., Geoly, A. D., Kratter, I. H. & Williams, N. R. Targeted neurostimulation reverses a spatiotemporal biomarker of treatment-resistant depression. *Proc. Natl Acad. Sci. USA* **120**, e2218958120 (2023).
72. Perez, D. L., Barsky, A. J., Vago, D. R., Baslet, G. & Silbersweig, D. A. A neural circuit framework for somatosensory amplification in somatoform disorders. *J. Neuropsychiatry Clin. Neurosci.* **27**, e40–e50 (2015).
73. Kim, S. M., Hong, J. S., Min, K. J. & Han, D. H. Brain functional connectivity in patients with somatic symptom disorder. *Psychosom. Med.* **81**, 313–318 (2019).
74. Liu, C.-H. et al. Increased salience network activity in patients with insomnia complaints in major depressive disorder. *Front. Psychiatry* **9**, 93 (2018).
75. Ihara, N. et al. Aberrant resting-state functional connectivity of the dorsolateral prefrontal cortex to the anterior insula and its association with fear avoidance belief in chronic neck pain patients. *PLoS ONE* **14**, e0221023 (2019).
76. Churchill, N. W., Hutchison, M. G., Graham, S. J. & Schweizer, T. A. Insular connectivity is associated with self-appraisal of cognitive function after a concussion. *Front. Neurol.* **12**, 653442 (2021).
77. Picon, E. L. et al. Memory perfectionism is associated with persistent memory complaints after concussion. *Arch. Clin. Neuropsychol.* **37**, 1177–1184 (2022).
78. Churchill, N. W., Hutchison, M. G., Graham, S. J. & Schweizer, T. A. Connectomic markers of symptom severity in sport-related concussion: whole-brain analysis of resting-state fMRI. *Neuroimage Clin.* **18**, 518–526 (2018).
79. Danielli, E. et al. A review of brain regions and associated post-concussion symptoms. *Front. Neurol.* **14**, 1136367 (2023).
80. Niu, X. et al. Disruption of periaqueductal grey-default mode network functional connectivity predicts persistent post-traumatic headache in mild traumatic brain injury. *J. Neurol. Neurosurg. Psychiatry* **90**, 326–332 (2019).
81. Kawabata, K. et al. Bridging large-scale cortical networks: integrative and function-specific hubs in the thalamus. *iScience* **24**, 103106 (2021).
82. Xu, H. et al. Neuroanatomical restoration of salience network links reduced headache impact to cognitive function improvement in mild traumatic brain injury with posttraumatic headache. *J. Headache Pain* **24**, 43 (2023).
83. Van Der Horn, H. J. et al. An integrated perspective linking physiological and psychological consequences of mild traumatic brain injury. *J. Neurol.* **267**, 2497–2506 (2020).

84. Smits, M. et al. Postconcussion syndrome after minor head injury: brain activation of working memory and attention. *Hum. Brain Mapp.* **30**, 2789–2803 (2009).
85. Mayer, A. R. et al. A functional magnetic resonance imaging study of cognitive control and neurosensory deficits in mild traumatic brain injury. *Hum. Brain Mapp.* **36**, 4394–4406 (2015).
86. Trapp, N. T. et al. Large-scale lesion symptom mapping of depression identifies brain regions for risk and resilience. *Brain* **146**, 1672–1685 (2023).
87. Eierud, C. et al. Neuroimaging after mild traumatic brain injury: review and meta-analysis. *Neuroimage Clin.* **4**, 283–294 (2014).
88. Cook, M. J. et al. Task-related functional magnetic resonance imaging activations in patients with acute and subacute mild traumatic brain injury: a coordinate-based meta-analysis. *Neuroimage Clin.* **25**, 102129 (2020).
89. Eickhoff, S. B. et al. Behavior, sensitivity, and power of activation likelihood estimation characterized by massive empirical simulation. *Neuroimage* **137**, 70–85 (2016).
90. Gilmore, C. S. et al. Deficits in visual system functional connectivity after blast-related mild TBI are associated with injury severity and executive dysfunction. *Brain Behav.* **6**, e00454 (2016).
91. Cash, R. F. H. et al. Personalized connectivity-guided DLPFC-TMS for depression: advancing computational feasibility, precision and reproducibility. *Hum. Brain Mapp.* **42**, 4155–4172 (2021).
92. Trapp, N. T., Pace, B. D., Neisewander, B., Ten Eyck, P. & Boes, A. D. A randomized trial comparing beam F3 and 5.5 cm targeting in rTMS treatment of depression demonstrates similar effectiveness. *Brain Stimul.* **16**, 1392–1400 (2023).
93. Cash, R. F. H. & Zalesky, A. Personalized and circuit-based transcranial magnetic stimulation: evidence, controversies, and opportunities. *Biol. Psychiatry* **95**, 510–522 (2024).
94. Fox, M. D. et al. Resting-state networks link invasive and noninvasive brain stimulation across diverse psychiatric and neurological diseases. *Proc. Natl Acad. Sci. USA* **111**, e4367–e4375 (2014).
95. Siddiqi, S. H. et al. Precision functional MRI mapping reveals distinct connectivity patterns for depression associated with traumatic brain injury. *Sci. Transl. Med.* **15**, eabn0441 (2023).
96. Davenport, N. D., Lim, K. O., Armstrong, M. T. & Sponheim, S. R. Diffuse and spatially variable white matter disruptions are associated with blast-related mild traumatic brain injury. *Neuroimage* **59**, 2017–2024 (2012).
97. Yeh, P. et al. Postconcussion disorder and PTSD symptoms of military-related traumatic brain injury associated with compromised neurocircuitry. *Hum. Brain Mapp.* **35**, 2652–2673 (2014).
98. King, N. S., Crawford, S., Wenden, F. J., Moss, N. E. G. & Wade, D. T. The Rivermead Post Concussion Symptoms Questionnaire: a measure of symptoms commonly experienced after head injury and its reliability. *J. Neurol.* **242**, 587–592 (1995).
99. McCarthy, P. FSLEYes. Zenodo <https://doi.org/10.5281/ZENODO.11047709> (2024).
100. PSaC Redo_Concussion studies only : 2025-06-10-15:27:48. NeuroVault <https://identifiers.org/neurovault.collection:20829> (2025).
101. NHLBI. Study Quality Assessment Tools (NIH, 2023).
102. Lancaster, J. L. et al. Bias between MNI and Talairach coordinates analyzed using the ICBM-152 brain template. *Hum. Brain Mapp.* **28**, 1194–1205 (2007).
103. Laird, A. R. et al. Comparison of the disparity between Talairach and MNI coordinates in functional neuroimaging data: validation of the Lancaster transform. *Neuroimage* **51**, 677–683 (2010).
104. Schaefer, A. et al. Local-global parcellation of the human cerebral cortex from intrinsic functional connectivity MRI. *Cereb. Cortex* **28**, 3095–3114 (2018).
105. Mollica, A. PsAc_ExtractedMNI_Excel. OSF https://osf.io/dpzmy/?view_only=4e9a8c80d37c464f98ba8cc7521a43d7 (2025).
106. Tse, N. Y., Ratheesh, A., Ganeshan, S., Zalesky, A. & Cash, R. F. H. Functional dysconnectivity in youth depression: systematic review, meta-analysis, and network-based integration. *Neurosci. Biobehav. Rev.* **153**, 105394 (2023).
107. IBM SPSS Statistics for Windows, version 29.0 (IBM Corp., 2022).
108. Eickhoff, S. B. et al. Coordinate-based activation likelihood estimation meta-analysis of neuroimaging data: a random-effects approach based on empirical estimates of spatial uncertainty. *Hum. Brain Mapp.* **30**, 2907–2926 (2009).
109. Eickhoff, S. B., Yeo, B. T. T. & Genon, S. Imaging-based parcellations of the human brain. *Nat. Rev. Neurosci.* **19**, 672–686 (2018).
110. Glasser, M. F. et al. The minimal preprocessing pipelines for the Human Connectome Project. *Neuroimage* **80**, 105–124 (2013).
111. Smith, S. M. et al. Resting-state fMRI in the Human Connectome Project. *Neuroimage* **80**, 144–168 (2013).
112. Cash, R. F. H., Müller, V. I., Fitzgerald, P. B., Eickhoff, S. B. & Zalesky, A. Altered brain activity in unipolar depression unveiled using connectomics. *Nat. Ment. Health* **1**, 174–185 (2023).
113. Cash, R. F. H. et al. Personalized brain stimulation of memory networks. *Brain Stimulat.* **15**, 1300–1304 (2022).
114. Fox, M. D., Liu, H. & Pascual-Leone, A. Identification of reproducible individualized targets for treatment of depression with TMS based on intrinsic connectivity. *Neuroimage* **66**, 151–160 (2013).

Acknowledgements

M.J.B. and S.M.N. were supported by the Kimel–Schatsky Traumatic Brain Injury Competition Grant from the Tory Trauma Program, Sunnybrook Research Institute. S.M.N. also received support from Brain Canada, the Canadian Institutes of Health Research (CIHR), and the Brain and Behavior Research Foundation. M.J.B. was supported by the Department of Psychiatry Academic Scholar Award at the University of Toronto. R.F.H.C. was supported by the National Health and Medical Research Council (NHMRC) Emerging Leadership Investigator Grant (2017527). A.M. and C.F.D.L. were supported by the Azrieli Brain Medicine Fellowship Program funded by The Azrieli Foundation. A.M., P.G., C.F.D.L., I.J.S., J.S.R., M.G., S.J.G., B.D., F.-H.L., N.L., C.H., M.J.B. and S.M.N. received support from the Harquail Centre for Neuromodulation and the Hurvitz Brain Sciences Program at the Sunnybrook Research Institute, Sunnybrook Health Sciences Centre.

Author contributions

A.M., R.F.H.C., M.J.B. and S.M.N. conceptualized the study. Methodology was developed by A.M., R.F.H.C., A.Z., M.J.B., and S.M.N. Software development was carried out by R.F.H.C. and A.Z., and R.F.H.C. also performed validation. Formal analysis was conducted by A.M., R.F.H.C. and S.M.N. Data curation was performed by A.M., C.F.D.L. and I.J.S. The original draft of the paper was written by A.M., R.F.H.C., M.J.B. and S.M.N. All authors contributed to review and editing of the paper. Visualization was performed by A.M. and R.F.H.C. Funding for the study was acquired by M.J.B. and S.M.N.

Competing interests

The authors declare no competing interests.

Additional information

Supplementary information The online version contains supplementary material available at <https://doi.org/10.1038/s44220-025-00503-6>.

Correspondence and requests for materials should be addressed to Sean M. Nestor.

Peer review information *Nature Mental Health* thanks Abel S. Mathew and the other, anonymous, reviewer(s) for their contribution to the peer review of this work.

Reprints and permissions information is available at www.nature.com/reprints.

Publisher's note Springer Nature remains neutral with regard to jurisdictional claims in published maps and institutional affiliations.

Open Access This article is licensed under a Creative Commons Attribution 4.0 International License, which permits use, sharing,

adaptation, distribution and reproduction in any medium or format, as long as you give appropriate credit to the original author(s) and the source, provide a link to the Creative Commons licence, and indicate if changes were made. The images or other third party material in this article are included in the article's Creative Commons licence, unless indicated otherwise in a credit line to the material. If material is not included in the article's Creative Commons licence and your intended use is not permitted by statutory regulation or exceeds the permitted use, you will need to obtain permission directly from the copyright holder. To view a copy of this licence, visit <http://creativecommons.org/licenses/by/4.0/>.

© The Author(s) 2025

¹Harquail Centre for Neuromodulation and Hurvitz Brain Sciences Program, Sunnybrook Research Institute, Toronto, Ontario, Canada. ²Department of Psychiatry, Sunnybrook Health Sciences Centre, University of Toronto, Toronto, Ontario, Canada. ³Systems Group, Department of Psychiatry, University of Melbourne, Melbourne, Victoria, Australia. ⁴Biomedical Engineering, University of Melbourne, Melbourne, Victoria, Australia. ⁵Department of Physical Medicine and Rehabilitation, St Luke's Medical Center, Bonifacio Global City, Philippines. ⁶Toronto Rehabilitation Institute, University Health Network, Toronto, Ontario, Canada. ⁷Rehabilitation Sciences Institute, University of Toronto, Toronto, Ontario, Canada. ⁸Physical Sciences Platform and Hurvitz Brain Sciences Program, Sunnybrook Research Institute, Toronto, Ontario, Canada. ⁹Department of Medical Biophysics, University of Toronto Faculty of Medicine, Toronto, Ontario, Canada. ¹⁰Division of Neurosurgery, Sunnybrook Health Sciences Centre, University of Toronto, Toronto, Ontario, Canada. ¹¹Division of Neurology, Department of Medicine, Sunnybrook Health Sciences Centre, University of Toronto, Toronto, Ontario, Canada.

¹²These authors contributed equally: Adriano Mollica, Robin F. H. Cash. ¹³These authors jointly supervised this work: Matthew J. Burke, Sean M. Nestor.

✉ e-mail: sean.nestor@utoronto.ca

Reporting Summary

Nature Portfolio wishes to improve the reproducibility of the work that we publish. This form provides structure for consistency and transparency in reporting. For further information on Nature Portfolio policies, see our [Editorial Policies](#) and the [Editorial Policy Checklist](#).

Statistics

For all statistical analyses, confirm that the following items are present in the figure legend, table legend, main text, or Methods section.

n/a Confirmed

- The exact sample size (n) for each experimental group/condition, given as a discrete number and unit of measurement
- A statement on whether measurements were taken from distinct samples or whether the same sample was measured repeatedly
- The statistical test(s) used AND whether they are one- or two-sided
 - Only common tests should be described solely by name; describe more complex techniques in the Methods section.*
- A description of all covariates tested
- A description of any assumptions or corrections, such as tests of normality and adjustment for multiple comparisons
- A full description of the statistical parameters including central tendency (e.g. means) or other basic estimates (e.g. regression coefficient) AND variation (e.g. standard deviation) or associated estimates of uncertainty (e.g. confidence intervals)
- For null hypothesis testing, the test statistic (e.g. F , t , r) with confidence intervals, effect sizes, degrees of freedom and P value noted
 - Give P values as exact values whenever suitable.*
- For Bayesian analysis, information on the choice of priors and Markov chain Monte Carlo settings
- For hierarchical and complex designs, identification of the appropriate level for tests and full reporting of outcomes
- Estimates of effect sizes (e.g. Cohen's d , Pearson's r), indicating how they were calculated

Our web collection on [statistics for biologists](#) contains articles on many of the points above.

Software and code

Policy information about [availability of computer code](#)

Data collection N/a

Data analysis N/a

For manuscripts utilizing custom algorithms or software that are central to the research but not yet described in published literature, software must be made available to editors and reviewers. We strongly encourage code deposition in a community repository (e.g. GitHub). See the Nature Portfolio [guidelines for submitting code & software](#) for further information.

Data

Policy information about [availability of data](#)

All manuscripts must include a [data availability statement](#). This statement should provide the following information, where applicable:

- Accession codes, unique identifiers, or web links for publicly available datasets
- A description of any restrictions on data availability
- For clinical datasets or third party data, please ensure that the statement adheres to our [policy](#)

The full meta-analytic output from the Neurosynth Compose analysis is publicly available at <https://identifiers.org/neurovault.collection:20829>. The dataset supporting the findings of this study (i.e., the full list of MNI coordinates extracted during the systematic review) is publicly available at https://osf.io/dpzmy/?view_only=4e9a8c80d37c464f98ba8cc7521a43d7.

Research involving human participants, their data, or biological material

Policy information about studies with [human participants or human data](#). See also policy information about [sex, gender \(identity/presentation\), and sexual orientation](#) and [race, ethnicity and racism](#).

Reporting on sex and gender

N/A

Reporting on race, ethnicity, or other socially relevant groupings

N/A

Population characteristics

N/A

Recruitment

N/A

Ethics oversight

N/A

Note that full information on the approval of the study protocol must also be provided in the manuscript.

Field-specific reporting

Please select the one below that is the best fit for your research. If you are not sure, read the appropriate sections before making your selection.

Life sciences Behavioural & social sciences Ecological, evolutionary & environmental sciences

For a reference copy of the document with all sections, see nature.com/documents/nr-reporting-summary-flat.pdf

Behavioural & social sciences study design

All studies must disclose on these points even when the disclosure is negative.

Study description

Multimodal neuroimaging meta-analysis

Research sample

Patients with persisting symptoms after concussion versus healthy controls

Sampling strategy

The sample used was based on available studies in the literature. The sample was representative.

Data collection

Systematic review searching available databases online. Studies for review and their data were collected in Excel.

Timing

Data collection began: March 2023. Data collection ended: September 2023

Data exclusions

No data were excluded from our analysis.

Non-participation

No participants were involved in this study.

Randomization

Not applicable as no participants were involved in this study.

Reporting for specific materials, systems and methods

We require information from authors about some types of materials, experimental systems and methods used in many studies. Here, indicate whether each material, system or method listed is relevant to your study. If you are not sure if a list item applies to your research, read the appropriate section before selecting a response.

Materials & experimental systems

- | | |
|-------------------------------------|--|
| n/a | Involved in the study |
| <input checked="" type="checkbox"/> | <input type="checkbox"/> Antibodies |
| <input checked="" type="checkbox"/> | <input type="checkbox"/> Eukaryotic cell lines |
| <input checked="" type="checkbox"/> | <input type="checkbox"/> Palaeontology and archaeology |
| <input checked="" type="checkbox"/> | <input type="checkbox"/> Animals and other organisms |
| <input checked="" type="checkbox"/> | <input type="checkbox"/> Clinical data |
| <input checked="" type="checkbox"/> | <input type="checkbox"/> Dual use research of concern |
| <input checked="" type="checkbox"/> | <input type="checkbox"/> Plants |

Methods

- | | |
|-------------------------------------|---|
| n/a | Involved in the study |
| <input checked="" type="checkbox"/> | <input type="checkbox"/> ChIP-seq |
| <input checked="" type="checkbox"/> | <input type="checkbox"/> Flow cytometry |
| <input checked="" type="checkbox"/> | <input type="checkbox"/> MRI-based neuroimaging |

Plants

Seed stocks

N/A

Novel plant genotypes

N/A

Authentication

N/A